Molecular Dynamics Study on Transport Properties of Fluids

Kazuo TOKIWANO† and Kiyoshi ARAKAWA*

Research Institute of Applied Electricity, Hokkaido University, Sapporo 060

†*Faculty of Engineering, Hokkaido University, Sapporo 060*

(Received November 13, 1980)

A molecular dynamics "experiment" has been performed for a system of 216 molecules interacting through a modified Lennard-Jones-type potential. The velocity autocorrelation functions and associated self-diffusion coefficients were computed for varying degrees of the steepness of the repulsive part in the pair potential. The dependence of these quantities upon the hardness of the core, and then the applicability of a perturbation approach to the transport theory, was elucidated. The computed self-diffusion coefficients were compared with the prediction of the Rice-Allnatt theory.

With the advent of computer experiment techniques, it has become possible to acquire useful information on dynamical processes in liquids by simulation. The velocity autocorrelation function $\Psi(t)$ is of particular interest, here, because it is the most important quantity for the description of the dynamics of liquids. Molecular dynamics experiments have been performed for the Lennard-Jones potential fluids by Rahman[1] and by Levesque-Verlet,[2] and, also for a rigid sphere fluid, those have been done by Alder-Wainwright and others.[3,4] The results have brought us some valuable information on $\Psi(t)$. Recent progress in the transport theory of liquids has been strongly promoted by these studies.[1-7]

The most important problem in the transport theory of liquids is to present a theoretical model amenable to the analytical treatment for various correlated motions of molecules in a liquid. In explaining the equilibrium properties of liquids, the perturbation approach has proved to be successful for the last decade.[8,9] The theory rests on the idea that the short range structure of liquids is governed primarily by a steep repulsive part of the intermolecular potential. Then, the attractive potential is regarded as a perturbation on a rigid sphere potential. Concerning transport properties, however, no successful perturbation theory has been proposed yet, and for the advancement of the theory, it is required to elucidate further the effect of the intermolecular potential upon the transport properties of fluids. Considerable efforts through computer experiments have been devoted to the presentation of a reference fluid, which is useful in predicting the transport properties of liquids. The predominant role of the repulsive interaction by hard cores in the dynamics of dense fluids has been confirmed through the molecular dynamics results.[6,10,11] Levesque *et al.*[2] stated that the transport coefficient for the Lennard-Jones fluids was practically explained in terms of a corresponding hard sphere model. On the other hand, concerning the effect of softness of the core, it seems that a soft core potential gives rise to remarked oscillations in $\Psi(t)$ while the diffusion coefficient is rather insensitive to the steepness of the repulsive core.[12] Then, for the elucidation of these properties of liquids, further examinations are required.

The purpose of the present work is to study the effect of the repulsive core on the transport properties of liquids with varying degrees of the steepness of the repulsive part of the potential. For that purpose, we consider a fluid system composed of molecules interacting through a modified Lennard-Jones-type potential: a parameter which shows the hardness of the repulsive core is introduced there. Velocity autocorrelation functions and associated self-diffusion coefficients for the systems are calculated by means of molecular dynamics experiments. The dependence of those quantities upon the hardness of the core and the applicability of a perturbation approach to the transport theory are investigated. Detailes of the results will be given in the following sections.

Molecular Dynamics Method

Description of the System. We consider a system composed of molecules interacting through a pair potential of the form

$$u(r_{ij}) = 4h\varepsilon\left[\left(\frac{\sigma}{r_{ij}}\right)^{12} - \left(\frac{\sigma}{r_{ij}}\right)^{6}\right] + (h-1)\varepsilon \quad r_{ij} \leq r_0$$
$$= 4\varepsilon\left[\left(\frac{\sigma}{r_{ij}}\right)^{12} - \left(\frac{\sigma}{r_{ij}}\right)^{6}\right] \quad r_{ij} > r_0, \quad (1)$$

where r_{ij} is the separation between molecules i and j, ε an energy parameter, and $r_0 = 2^{1/6}\sigma$. This potential function has a minimum of $-\varepsilon$ at r_0 and crosses the abscissa at the distance σ_0, and

$$\sigma_0 = [2(h - \sqrt{h})/(h-1)]^{1/6}\sigma \quad h \neq 1$$
$$= \sigma \quad h = 1. \quad (2)$$

h is a parameter which shows the hardness of the repulsive core. When $h=1$, $u(r_{ij})$ becomes a Lennard-Jonse 12-6 potential with parameters ε and σ. Figure 1 displays the potential curves for different values of h for the same ε and σ (Fig. 1-(a)) and those for the same ε and σ_0 (Fig. 1-(b)). For large values of h the potential may be regarded as a nearly rigid sphere potential with an attractive part.

Reduced quantities have been used throughout. There is some arbitrariness in choosing the reduction units for the present potential system. We have taken the reduced density ρ^* and the reduced temperature T^* as

$$\rho^* = N\sigma_0^3/V \text{ and } T^* = kT/\varepsilon, \quad (3)$$

respectively, where k is the Boltzmann constant.

The magnitude of ρ^* of the systems considered were taken to be not larger than 0.95. When exceeded this reduced density, the system actually lost its fluidity for the lowest temperature chosen, showing an adrupt

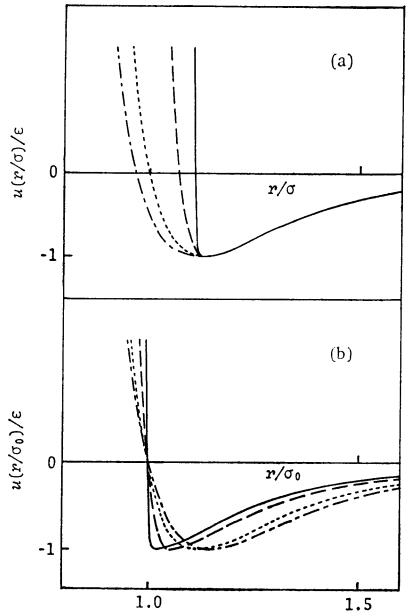

Fig. 1. Intermolecular potentials for varying degrees of the steepness of the repulsive potential.
(a): For constant ε and σ, (b): for constant ε and σ_0.
——: $h=200$, – – –: $h=10$, ·····: $h=1$, —·—: $h=0.5$.

drop in the diffusion coefficient. With respect to temperature, we have taken the range of T^* of 0.6—4.0, because we consider the liquids composed of molecules interacting with comparatively strong forces, such as H_2O, C_6H_6, CCl_4, CH_3OH *etc.*[13]

Computational Technique. Molecular dynamics calculations have been performed for the system of 216 molecules confined to a cubic box with volume V, interacting through the potential Eq. 1. Following the usual procedure in molecular dynamics studies, the periodic boundary conditions were employed and interactions beyond a cutoff distance r_c were ignored. The cutoff was placed at $r_c=2.5\,\sigma_0$. The technique due to Verlet[15] was used to integrate the $3N$ coupled Newton equations of motion,

$$m\frac{\mathrm{d}^2\boldsymbol{r}_i}{\mathrm{d}t^2} = -\boldsymbol{\nabla}_i\sum_{i\neq j}^{N}u(r_{ij}). \tag{4}$$

The basic time increment for the numerical integration has been taken to be 0.012 (in $(m\sigma_0^2/\varepsilon)^{1/2}$), taking the conservation of total energy of the system into account. The number of time steps required to investigate a given thermodynamic state was about 12000 time steps; 2000 time steps were sufficient, usually, to reach equilibrium, and a period of 10000 time steps was utilized to form the statistical average. The results were stable and reproducible.

Radial Distribution Function. The radial distribution function gives the average local density of molecules at distance r from the central molecule, and is indicative of the local structure in a liquid.

Figure 2 displays the computed radial distribution functions, $g(r^*)$, *vs.* $r^*=r/\sigma_0$ at $\rho^*=0.80$ for varying h, including the result of Alder and Hecht on rigid spheres.[16] It is seen that the curve for $h=200$ agrees closely with that for the rigid spheres. As the softness

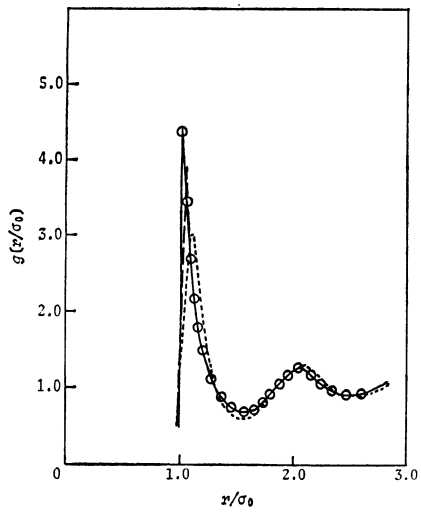

Fig. 2. Radial distribution functions at $\rho^*=0.80$ and $T^*\simeq 0.6$.
——: $h=200$, – – –: $h=10$, ·····: $h=1$, ○: rigid spheres for $V/V_0=1.7$ given by Alder and Hecht.[16]
Refer to Fig. 1-(b) for the potentials.

of the repulsive core increases, the first peak of the distribution function is less sharp.[12,17] The $g(r^*)$ for $h=1$ can be compared with the distribution function of liquid Ar.[18] These results show the effectiveness of the present potential function.

Velocity Autocorrelation Function

The normalized velocity autocorrelation function at time t has been calculated as

$$\Psi(t) = \frac{\langle \boldsymbol{v}(0)\cdot\boldsymbol{v}(t)\rangle}{\langle v^2\rangle} = \frac{\langle \frac{1}{N}\sum_i^N \boldsymbol{v}_i(t_0)\cdot\boldsymbol{v}_i(t_0+t)\rangle_{t_0}}{\langle \frac{1}{N}\sum_i^N \boldsymbol{v}_i(t_0)\cdot\boldsymbol{v}_i(t_0)\rangle_{t_0}}, \tag{6}$$

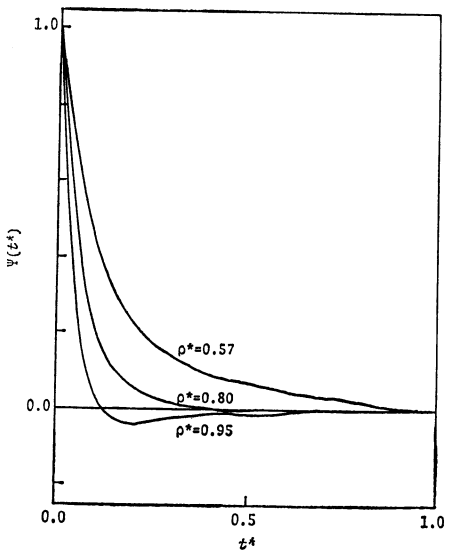

Fig. 3. Velocity autocorrelation functions for $h=200$ at $T^*\simeq 1.0$.

where $v_i(t)$ is the linear velocity of a molecule i at t, and the angular brackets $< >_{t_0}$ imply a mean value over time origins.

For a short time behavior of $\Psi(t)$, we have made a comparison of molecular dynamics computations with the values given by the Brownian and Gaussian approximations (see Appendix I).

Figure 3 shows the normalized velocity autocorrelation functions, $\Psi(t^*)$, computed by means of Eq. 6 for various values of ρ^* for $h=200$ and $T^*=1$, where t^* is the reduced time given by $t^*=t/(m\sigma_0^2/\varepsilon)^{1/2}$. The statistical error on the normalized velocity autocorrelation function is due mainly to the replacement of an equilibrium ensemble average by a time average over a finite time interval. In the present case, the error is estimated to be $\pm 0.015|\Psi(t)-1|$ by means of Zwanzig and Ailawadi's formula.[19]

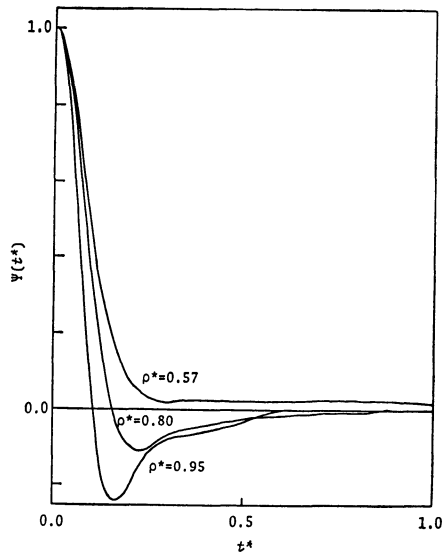

Fig. 4. Velocity autocorrelation functions for $h=1$ at $T^*\simeq 0.6$.

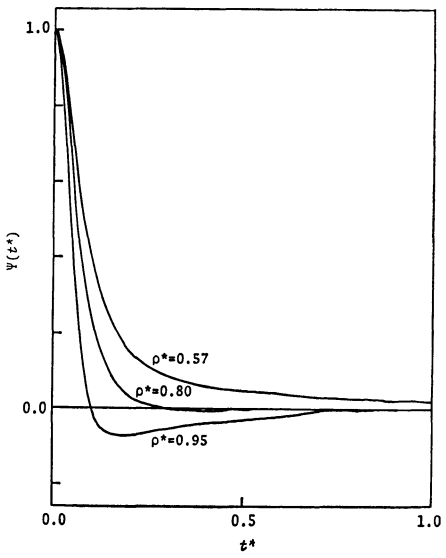

Fig. 5. Velocity autocorrelation functions for $h=10$ at $T^*\simeq 0.6$.

At low density $\Psi(t^*)$ decays steadily. When the density is higher, $\Psi(t^*)$ has a pronounced minimum attributed to the "back-scattering" of the diffusing molecule due to its collisions with surrounding molecules,[1,10] followed by a negative plateau. The level of the negative region rises up with decreasing density, becoming eventually positive at a low density. The qualitative behavior of $\Psi(t^*)$ is consistent not only with Alder and Wainwright's[4] computer results on rigid spheres but also with Levesque and Verlet's[2] results on the Lennard-Jones fluid.

We now examine the effect of the steepness of the repulsive core potential on the velocity autocorrelation function. Figures 4—9 present $\Psi(t^*)$ computed at the same reduced temperature ($T^*=0.6$) and different densities, for $h=0.1$, 0.5, 1, 10, and 200. The results

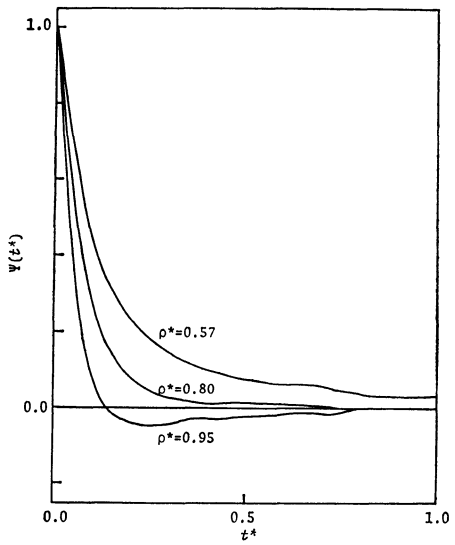

Fig. 6. Velocity autocorrelation functions for $h=200$ at $T^*\simeq 0.6$.

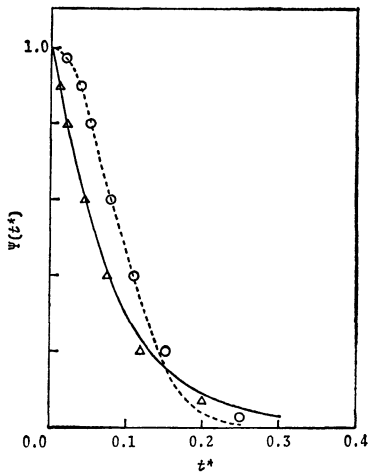

Fig. 7. Comparison of the velocity autocorrelation functions computed by molecular dynamics at $\rho^*=0.80$ and $T^*\simeq 0.6$ with those predicted by Brownian and Gaussian approximations.
△: $h=200$ by MD, ——: $h=200$ by Brownian approx. (Eq. AI-1), ○: $h=1$ by MD, ·····: $h=1$ by Gaussian approx. (Eq. AI-4). Refer to Fig. 1-(b) for the potentials.

are summarized as in the following (1)—(4).

(1) At short times, $\Psi(t^*)$ for large values of h has an appearence of the exponential or nearly exponential decay (Fig. 6). When h becomes smaller, the initial behavior of $\Psi(t^*)$ shows an extended Gaussian appearence (Fig. 4). The extent of the Gaussian decay at a soft core system can be understood intuitively as the effect of the duration of a collision. This is more clearly seen in Fig. 7. The figure displays the $\Psi(t^*)$ computed for the soft core ($h=1$), together with the curve predicted by the Gaussian approximation (Eq. AI-4), and also that for the hard core ($h=200$) with the curve obtained from the Brownian approximation (Eq. AI-1). The agreement between the computed and predicted values is very good.[20] It is confirmed that the initial decay of $\Psi(t^*)$ for $h=200$ is still Gaussian at extremely short times. The initial purely-Gaussian decay is attributed to a quasi-Brownian motion of the pair of molecules in the relatively weak, but rapidly fluctuating, field of all the neighboring molecules, in which the momentum transfer is understood to be small.[21]

(2) At intermediate times, $\Psi(t^*)$ at high density has a negative region with a long plateau. As seen in Figs. 4—6, the soft core potential has an effect enhancing the negative correlations. $\Psi(t^*)$ for large h shows the overdamped behavior and no oscillatory features. The oscillatory aspect of the self motion associated with the soft core is very weak in the Lennard-Jones case (Fig. 4). However, as Fig. 8 shows, $\Psi(t^*)$ of $h=0.1$ apparently shows the oscillatory behavior similar to that found in molecular dynamics experiments on liquid metals[12] and also has no longer an appreciably long plateau. The long plateau is not a consequence of an attractive potential tail but an essential feature for rigid sphere systems; it is generally believed to arise from repeated collisions between the two molecules due to the cage effect of its neighbors.[22]

(3) As seen in Fig. 9, when h increases at the same reduced density, the behavior of $\Psi(t^*)$ approaches that of $\Psi(t^*)$ for rigid spheres. The area under $\Psi(t^*)$ increases at small times with increasing softness of the core, but at intermediate times we observe an opposite trend on $\Psi(t^*)$ throughout three cases (a) ($\rho^*=0.57$), (b) ($\rho^*=0.85$), and (c) ($\rho^*=0.95$). In this respect, the three groups of curves given in Figs. 9(a), (b), and (c) may be said to have a similar trend of change with the increase of h over all the range of t^*. The decrease of $\Psi(t^*)$ at intermediate times is largely compensated for by its increase at small times. This is the reason why the self-diffusion coefficient, which is given by the integral of $\Psi(t)$, is rather insensitive to the shape of intermolecular potentials (Table 1). Figure 10 shows $\Psi(t^*)$ for varying h at $T^*=1.0$. The trend of change

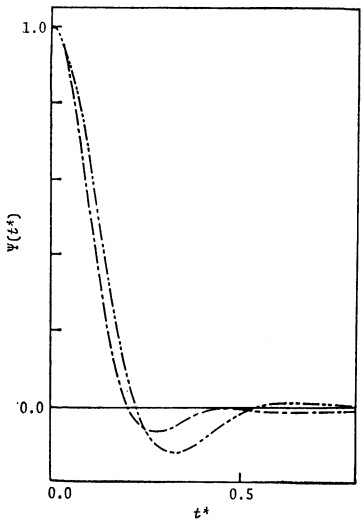

Fig. 8. Velocity autocorrelation functions for $h<1$ at $\rho^*=0.70$ and $T^*\simeq 0.6$.
——: $h=0.5$, ----: $h=0.1$. Refer to Fig. 1-(b) for the potentials.

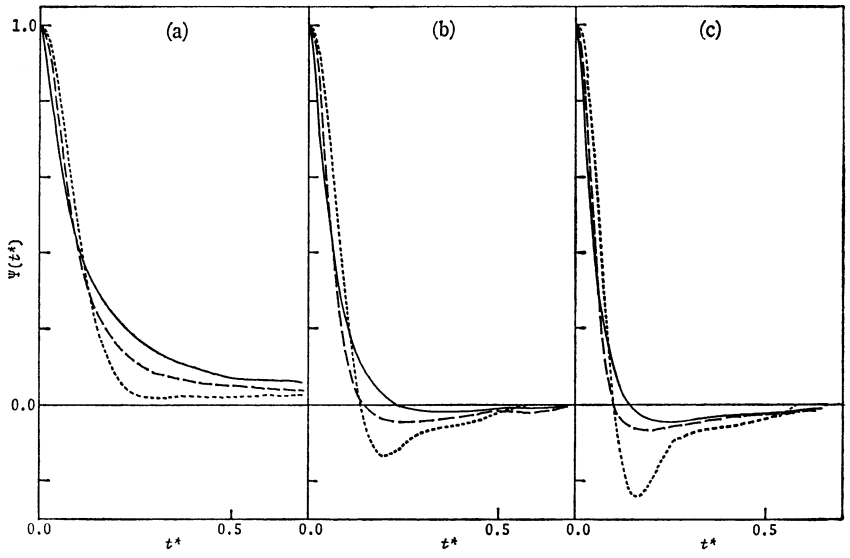

Fig. 9. Velocity autocorrelation functions for potential functions presented in Fig. 1-(b) at $T^*\simeq 0.6$.
(a): For $\rho^*=0.57$, (b): for $\rho^*=0.85$, (c): for $\rho^*=0.95$. ——: $h=200$, ----: $h=10$, ……: $h=1$.

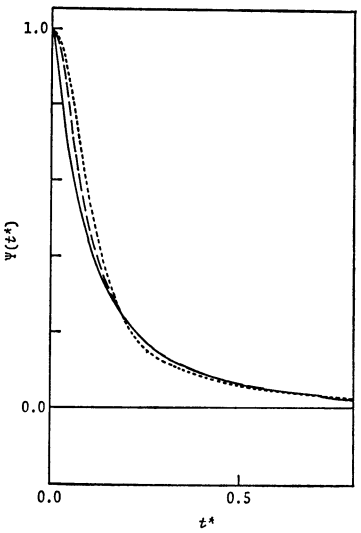

Fig. 10. Velocity autocorrelation functions at $\rho^*=0.57$ and $T^*=1.0$.
——: $h=200$, ----: $h=10$, ·····: $h=1$.

with the increasing h is found to be essentially similar to that at $T^*=0.6$, though its magnitude is small.

The fundamental behavior of velocity autocorrelation functions for continuous potential fluids may be explained by the extreme one of rigid spheres with an appropreate diameter at the same volume. The existence of such an extreme offer the basis of a perturbation approach in the transport theory. In Fig. 9 we have used simply σ_0 as a diameter of rigid spheres as a reference. A useful way to determine the rigid core diameter will be the one due to Dymond and Alder.[10]

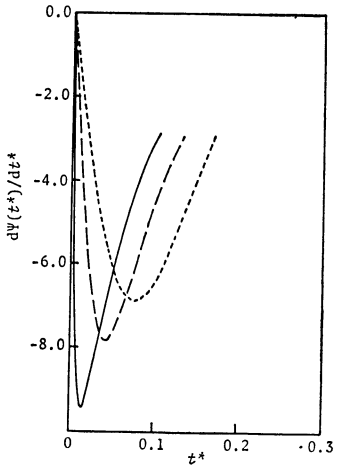

Fig. 11. First derivatives of the velocity autocorrelation functions at $\rho^*=0.57$ and $T^*\simeq 0.6$.
——: $h=200$, ——: $h=10$, ·····: $h=1$. Refer to Fig. 1-(b) for the potentials.

(4) We present the first derivative $d\Psi(t^*)/dt^*$ in the region of initially fast decay for varying h in Fig. 11. The first minimum point of $d\Psi(t^*)/dt^*$ *vs.* t^* curves, or the first inflexion point of $\Psi(t^*)$ *vs.* t^* curves, gives the time at which the force autocorrelation function first passes through zero. As Fig. 11 shows, that is strongly dependent on the steepness of the core potential, going to zero as a rigid core limit as h becomes large.[23] The decay time of $\Psi(t^*)$ appears to be relatively insensitive to the steepness of the repulsive core potential in spite of the strong dependence of the force autocorrelation. This implies that the motion of a molecule in the systems considered is far from harmonic oscillations.

Here, we would mention the following point. The extreme of $h=\infty$ in the present potential may be closer to a square-well potential for the presence of an attractive part rather than to rigid spheres (see Fig. 1). The velocity autocorrelation functions for square-well potential fluids have been calculated by Michels and Trappeniers.[24] Unfortuately, their molecular dynamics calculations were made at too low densities to confirm the velocity autocorrelation at liquid densities. Einwohner and Alder[25] computed the free-path distributions and collision rates in square-well potential fluids as well as those in rigid sphere fluids, and made the comparison between the two cases. They found that at liquid density the majority of collisions were hard core collisions and the free-path distribution was nearly indifferent to the presence of an attractive potential. For the extreme of $h=\infty$ in the present potential, the velocity autocorrelation function is supposed to be approximately equal to the one for rigid spheres, except for low densities.

Self-diffusion Coefficient

Procedure of Calculations. The self-diffusion coefficient D is calculated either from the velocity autocorrelation function,

$$D=\frac{kT}{m}\int_0^\infty \Psi(t)\mathrm{dt}, \tag{7}$$

or from the long time limit of the mean-square displacement of a selected molecule i,

$$D=\lim_{t\to 0}\left[\frac{1}{6t}<[\boldsymbol{r}_i(0)-\boldsymbol{r}_i(t)]^2>\right]. \tag{8}$$

The evaluation of integral in Eq. 7 was carried out over the range of t, 0—2000 time steps. In the application of Eq. 8, we used the slope of the linear part of the curve for the mean-square displacement at 2000 time steps. The error of both results are considered to be of the order of 10%, and then, both results may be safely said to agree to each other within the range of errors. The diffusion coefficient for liquid Ar (at 94 °K and 1.374 g cm^{-3}) was calculated to be 2.44×10^{-5} cm^2 s^{-1} in agreement with Rahman's result.[1]

The self-diffusion coefficients, D_{MD}, calculated from the velocity autocorrelation function are listed in Table 1, where we have used as the reduced quantity

$$D^*=D/(\sigma_0^2\varepsilon/m)^{1/2}. \tag{9}$$

We can not make a direct comparison of the values for $h=1$ with the results of Levesque and Verlet[2] on the Lennard-Jones fluid. It is possible to compare those by the use of $(\sigma^2\varepsilon/m)^{1/2}(kT/\varepsilon)^{5/12}$ as a unit of D and $\rho'=(\rho\sigma^3/\sqrt{2})(\varepsilon/kT)^{1/4}$ as the reduced density.[26] Both results are confirmed to be quite similar each other

Table 1. Self-diffusion coefficients

ρ^*	h	T^*	D_{MD}^*
0.42	1	0.61	0.084
0.51	10	0.61	0.094
0.57	1	0.60	0.072
0.57	10	0.61	0.085
0.57	200	0.60	0.101
0.57	200	0.99	0.143
0.57	200	4.01	0.430
0.59	1	0.61	0.067
0.70	1	0.59	0.055
0.72	10	0.61	0.067
0.80	1	0.61	0.029
0.80	10	0.59	0.041
0.80	50	0.60	0.042
0.80	100	0.60	0.049
0.80	200	0.59	0.050
0.80	200	0.99	0.061
0.80	200	3.94	0.148
0.86	10	0.60	0.022
0.95	1	0.61	0.006
0.95	10	0.60	0.011
0.95	200	0.59	0.016
0.95	200	1.02	0.022
0.95	200	3.97	0.064

except for those at the low density ($\rho'<0.55$), showing that the scaling variables for the inverse 12-th power potential may be useful for the Lennard-Jones fluids.

Density Dependence of Self-Diffusion Coefficient. Figure 12 illustrates the density dependence of the self-diffusion coefficients at $T^*=0.6$ for a variety of the steepness of core potentials. The curves are found to shift along an arrow in the figure, when the hardness of the repulsive core increases.

We now attempt here an interpretation of this result by means of a rigid sphere model. The self-diffusion coefficient for rigid sphere gas of packing fraction

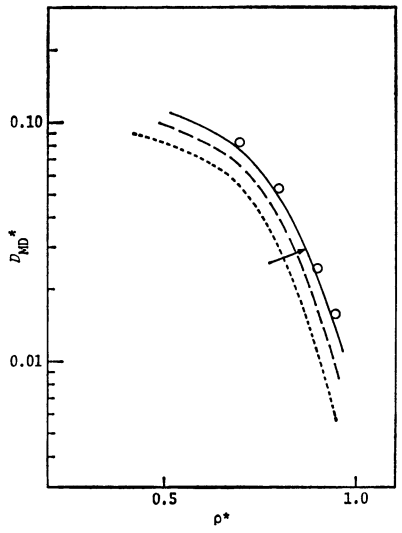

Fig. 12. Density dependence of self-diffusion coefficients at $T^*\simeq 0.6$.
——: $h=200$, ——: $h=10$, ·····: $h=1$, ○: D_∞^* calculated by means of Eq. 11.

$\xi(=(\pi/6)\rho d^3)$, where d is the diameter of spherical molecules, is given by the Enskog theory as

$$D_E=\frac{3}{8}\frac{1}{\rho d^2}\left(\frac{kT}{\pi m}\right)^{1/2}\Big/\left[\frac{3}{2\pi\rho d^3}(\chi(\xi)-1)\right], \qquad (10)$$

in which $\chi(\xi)$ $(=pV/NkT)$ is the compressibility factor of a rigid sphere system. We consider the extreme of $h=\infty$ in the present potential *i.e.* the nearly rigid sphere potential with an attractive potential well. Let us assume that the self-diffusion coefficient for the system is given by the Enskog's value corrected by the Alder-Wainwright factor as the ratio $(D_{MD}^H/D_E)_A$,[3,4] where D_{MD}^H is the molecular dynamics values of diffusion coefficients for rigid spheres. It is written as[2]

$$D_\infty^*=\frac{(\sqrt{\pi}/4)\sqrt{T^*}}{\chi(\xi)-1}\left(\frac{D_{MD}^H}{D_E}\right)_A, \qquad (11)$$

where D_∞^* is expressed as the reduced coefficient given by Eq. 9. $\chi(\xi)$ is given by the formula $\chi(\xi)=(1+\xi+\xi^2)/(1-\xi)^3$. D_∞^* calculated at $T^*=0.6$ are plotted against ρ^* in Fig. 12. We can see that the D_{MD}^* *vs.* ρ^* curve for $h=200$ nearly agrees with the D_∞^* *vs.* ρ^* one. That is, when the hardness of the core increases, the D_{MD}^* *vs.* ρ^* curve at a given temperature, shifting along the arrow in Fig. 12, approaches the extreme curve of rigid spheres at the same temperature. This confirms that the rigid sphere model expressed as Eq. 11 gives a good description of self-diffusion coefficients for realistic continuous potential systems. An appropriate evaluation of the equivalent rigid sphere diameter for the Lennard-Jones fluid was given by Verlet,[18] who took for it the value to fit the equilibrium structure factor to the Wertheim-Thiele solution of the PY equation for rigid spheres. Using the core diameter thus determined, Levesque *et al.*[2] calculated diffusion coefficients for Lennard-Jones fluids, which were found to be about 10% larger than those by molecular dynamics computations. According to Verlet,[18] at low temperatures, the equivalent diameter is larger than the original core size σ in the Lennard-Jones potential. The direction of the arrow in Fig. 12 is consistent with the result of Verlet.

In addition to the interpretation described above, it can also be said from Fig. 12 that the duration of collisions between molecules, associated with the finite steepness of the repulsive potential, brings an important perturbation on the dynamical behavior of molecules mainly determined by the rigid sphere potential.

Comparison with the Rice-Allnatt Theory. The basic assumption underlying the transport theory of Rice and Allnatt[21] is that the motion of a molecule in a fluid consists of a strongly repulsive binary encounter followed by a quasi-Brownian motion of the molecules in the fluctuating field of neighboring molecules. The successive repulsive encounters are assumed to occur independently. This assumption is in direct opposition to the van der Waals picture of transport processes discussed by Dymond and Alder and others,[10] in which the dynamical event consists of correlated collisions of rigid spheres. The real situation lies between these two extremes, probably.

We attempt here to test the Rice-Allnatt theory through the examination of self-diffusion coefficients

calculated for various degrees of the steepness of the repulsive potential.[27] In the theory,

$$V(r) = V^{H}(r) + V^{S}(r)$$
$$\begin{cases} V^{H}(r) = \infty, \quad V^{S}(r) = 0 & r \leq a \\ V^{H}(r) = 0 & r > a, \end{cases} \tag{12}$$

where V^S is the soft potential. The forces on the molecules in a liquid are working on two time scales: one corresponds to the large momentum and energy transfers which occur during rigid sphere collisions, and the other to the frequent small momentum transfers which occur during the quasi-Brownian motion of a molecule in the soft force field. Then, the friction coefficient is expressed as $\zeta=\zeta^H+\zeta^S$, and the self-diffusion coefficient is

$$D_{RA} = \frac{kT}{\zeta^H+\zeta^S}, \tag{13}$$

where the friction coefficients become

$$\zeta^H = \frac{8}{3}(\pi mkT)^{1/2}\rho a^2 g(a), \tag{14}$$

and

$$\zeta^S = -\frac{16\pi^4}{3}\rho\left(\frac{\pi m}{kT}\right)^{1/2}\int_0^\infty dq\, q^3 V_q^S G_q. \tag{15}$$

The Fourier transforms V_q^S and G_q are given by

$$V_q^S = \frac{1}{8\pi^3}\int d\boldsymbol{r}\, e^{-i\boldsymbol{q}\cdot\boldsymbol{r}} V^S(r), \tag{16}$$

and

$$G_q = \frac{1}{8\pi^3}\int d\boldsymbol{r}\, e^{-i\boldsymbol{q}\cdot\boldsymbol{r}}(g(r) - 1), \tag{17}$$

respectively. The rigid core contribution, Eq. 14, is the Enskog expression. The evaluation of ζ^S, Eq. 15, is identical with the friction coefficient given by Helfand by applying the linear trajectory approximation.[29] For the application of the Rice-Allnatt theory to the present system, there is obviously some arbitrariness in choosing the core diameter a in Eq. 12. In this work, the distance where the potential crosses abscissa has been taken as the diameter. Equation 1 is rewritten as follows,

$$V^H(x) = \infty, \quad V^S(x) = 0 \qquad x \leq x_0$$
$$V^H(x) = 0, \quad V^S(x) = u(\sigma x) \quad x > x_0, \tag{18}$$

where $x=r/\sigma$ and $x_0=\sigma_0/\sigma$.

It is difficult to calculate ζ^S using Eq. 15 because of the presence of the factor q^3 and the oscillating behavior due to G_q in the integrand. However, for the present potential (Eq. 18) we can invert Eq. 15 according to the procedure used by Helfand. The details of the inversion are described in Appendix II. If we use the dimensionless coefficient $\zeta_r^S=\zeta^S/\zeta^*$ where $\zeta^*=(8/3)\rho x_0^2(\pi mkT)^{1/2}$, ζ_r^S is given by

$$\zeta_r^S = \left(\frac{\varepsilon}{kT}\right)\int_{x_*}^\infty dx f(x)\,(g(\sigma x) - 1) - \left(\frac{\varepsilon}{kT}\right)\int_0^{x_*} dx f(x), \tag{19}$$

and

$$f(x) = (1-h)\left[\frac{11}{2^{11/6}}f_{12}\left(\frac{x}{2^{1/6}}\right) - \frac{5}{2^{5/6}}f_6\left(\frac{x}{2^{1/6}}\right)\right] + h\left[\frac{11}{x_0^{11}}f_{12}\left(\frac{x}{x_0}\right) - \frac{5}{x_0^5}f_6\left(\frac{x}{x_0}\right)\right], \tag{20}$$

where

$$f_n(x) = 2\sum_{j=1}^{n/2}\frac{x^{2j-1}}{2j-1} - x^{1-n}\ln\left|\frac{x+1}{x-1}\right|. \tag{21}$$

Table 2. Friction and self-diffusion coefficients given by the Rice-Allnatt theory at $T^*\simeq 0.6$

	ρ^*	ζ_r^H	ζ_r^S	$\zeta_{RA,r}$	D_{RA}^*	$\zeta_{MD,r}$
$h=1$	0.57	0.85	4.48	5.33	0.054	4.03
	0.59	0.94	4.38	5.32	0.052	4.16
	0.70	0.69	3.86	4.55	0.051	4.21
	0.80	0.89	3.84	4.73	0.031	5.02
	0.95	1.51	3.97	5.48	0.032	29.56
$h=10$	0.57	0.90	7.17	8.09	0.050	4.74
	0.72	0.72	6.53	7.25	0.032	3.40
	0.80	0.85	7.16	8.01	0.025	8.01
	0.86	0.90	7.32	8.22	0.024	8.82
	0.95	1.24	8.15	9.39	0.018	15.50
$h=200$	0.57	0.81	22.60	23.41	0.013	2.86
	0.80	0.80	22.43	23.23	0.009	4.04
	0.95	1.17	27.11	28.28	0.009	15.21

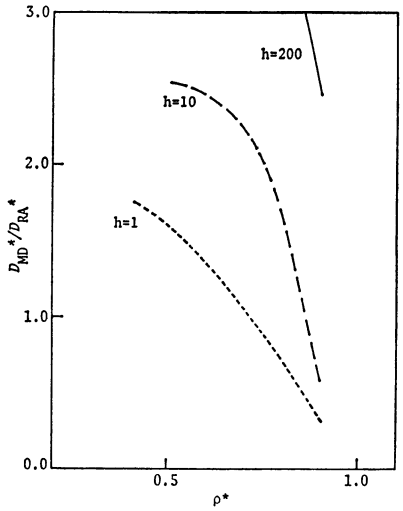

Fig. 13. Ratio of the values of self-diffusion coefficients at $T^*\simeq 0.6$ calculated by molecular dynamics to those predicted by the Rice-Allnatt thery.

$\zeta_r^H(=\zeta^H/\zeta^*)$, ζ_r^S, and D_{RA}^* are calculated by means of Eqs. 14, 19, and 13, respectively, using the radial distribution functions calculated by the molecular dynamics runs for the potential Eq. 1.[30] The results are given in Table 2, together with the molecular dynamics computations, $\zeta_{MD,r}^*(=(kT/D_{MD})/\zeta^*)$.

Figure 13 shows the D_{MD}^*/D_{RA}^* *vs.* ρ^* curves, for $h=1$, 10, and 200. As seen in Table 2 and Fig. 13, a good agreement between the predicted and computed values is obtained only for the Lennard-Jones potential ($h=1$) at a moderate density and also for the more rigid potential ($h=10$) at a high density. Too small values of D_{RA}^* for large h are evidently attributed to the overestimation of ζ_r^S about the contributions of the repulsive part, including the improperly strong repulsive contribution. The prediction of the Rice-Allnatt theory using the linear trajectory procedure is found to depend too sensitively upon how to separate the intermolecular potential. We have taken the diameter of rigid core to be equal to σ_0.

It is found from Fig. 13 that the ratio D_{MD}^*/D_{RA}^* for $h=1$ is smaller than 1 at high densities, and at low

densities we have an opposite result. This density dependence of the ratio D_{MD}^*/D_{RA}^* is supposed to be partly associated with that of the Alder-Wainwright ratio $(D_{MD}^H/D_E)_A$ for rigid spheres.

Concluding Remarks

By means of molecular dynamics calculations, we have examined the transport properties of a fluid composed of molecules interacting through the potential expressed in terms of three parameters: the depth of potential well ε, core size σ_0, and hardness parameter h. The results are summarized as follows.

(a) The essential feature of the behavior of velocity autocorrelation functions for continuous potential fluids can be explained by the extreme of rigid spheres with an appropriate diameter at the same volume. This implies that the rigid-sphere fluid can serve as a reference system suitable for the representation of dynamical properties of liquids.

(b) The detailed behavior of velocity autocorrelation functions is sensibly dependent upon the steepness of the repulsive core potential. The oscillatory behavior superimposed on the extreme behavior of rigid spheres becomes more pronounced as the softness of the core increases. Then, the decrease of the area under $\Psi(t)$ at intermediate times is largely compensated for by its increase at small times. This is the reason why the self-diffusion coefficient is rather insensitive to the shape of intermolecular potentials.

(c) The density dependence curve of self-diffusion coefficients in a continuous potential fluid shifts and approaches to that of rigid spheres at the same temperature with the increasing hardness of the core.

These results appear to offer a sound basis for the equivalent hard sphere model as well as for the applicability of the perturbation approach to the transport theory. The idea of separating the intermolecular potential into a rigid core part and a soft one, treating the latter as a perturbation, is considered to be essentially applicable to the transport theory of liquids. This is the basic physical assumption underlying the generalized van der Waals theory[10,31] and the dynamical model of liquids due to Rice and Allnatt. The results calculated by the use of the Rice-Allnatt model are also found to be strongly dependent of the arbitrariness in splitting the potential into two parts. At high densities and low temperatures, the correlated successive rigid core collisions of a pair of molecules is considered to have more important effects on the self-diffusion coefficients.

Appendix I

A Langevin type of velocity autocorrelation function arising from a Markovian velocity evolution is expressed as

$$\Psi(t) = \exp\left(-\frac{kT}{mD}t\right), \tag{AI-1}$$

where D is a self-diffusion coefficient. Equation AI-1 is expected to give a good description to $\Psi(t)$ for a hard core potential (large h) at a moderate density. It is evident that $\Psi(t)$ for a soft core potential (small h) is far from the simple exponential behavior. If the interaction potential is a smooth function where there is no rigid core, then $\Psi(t)$ can be assumed to be analytical in the neighborhood of $t=0$ and expanded in a Taylor series

$$\Psi(t) = 1 - \frac{\omega_e^2}{2!}t^2 + O(t^4), \tag{AI-2}$$

where the square of the Einstein frequency, ω_e^2, is given in terms of the average of the Laplacian of the total potential energy U:

$$\omega_e^2 = \frac{\langle v^2 \rangle}{\langle v^2 \rangle} = \frac{1}{3m}\langle \nabla^2 U \rangle. \tag{AI-3}$$

Then, the Gaussian decay of $\Psi(t)$ is given by

$$\Psi(t) \simeq \exp\left[-\frac{\langle \nabla^2 U \rangle}{6m}t^2\right]. \tag{AI-4}$$

Since the potential function, Eq. 1, is continuous, the slope of $\Psi(t)$ at $t=0$ is zero and the decay at a small time should be Gaussian even for large values of h. For a completely rigid core, however, collisions are instantaneous and this results in a cusp of $\Psi(t)$ at $t=0$.

Appendix II

The inversion of the transforms in Eq. 15 can be made according to the same procedure as used by Helfand.[29] Equation 16 is integrated by parts to give

$$V_q^S = \frac{1}{2\pi^2}\int_0^\infty dq \frac{\cos(qr)}{q^2}\frac{d}{dr}[rV^S(r)]. \tag{AII-1}$$

Substitution of Eq. AII-1 into Eq. 15 gives

$$\zeta_r^S = -\frac{1}{4\sigma^2}\frac{1}{kT}\int_0^\infty dq \int_0^\infty dr \int_0^\infty dr' r' [\sin q(r'+r) + \sin q(r'-r)] \times [g(r') - 1]\frac{d}{dr}[rV^S(r)], \tag{AII-2}$$

Using the relation $\int_0^\infty \sin(qr)dq = p/r$, where p stands for the principal part, and introducting the change of variables $y = r/r'$ and $x = r'/\sigma$, we obtain from the integration over q of Eq. AII-2

$$\zeta_r^S = -\frac{1}{4}\frac{1}{kT}\int_0^\infty dx \int_{x,/x}^\infty dy \left(\frac{p}{1+y} + \frac{p}{1-y}\right) x \frac{d}{dy} [yV^S(\sigma xy)][g(\sigma x) - 1]. \tag{AII-3}$$

For the potential function given by Eq. 18, Eq. AII-3 can be integrated over y explicitly to lead

$$\zeta_r^S = \left(\frac{\varepsilon}{kT}\right)\int_0^\infty dx f(x)[g(\sigma x) - 1], \tag{AII-4}$$

where $f(x)$ is given by Eq. 20. When $h=1$ and hence $x_0=1$, Eq. AII-4 is reduced to the expression of Helfand. Since $g(\sigma x)$ vanishes in the region $0 < x < x_0$, Eq. AII-4 is rewritten as Eq. 19.

We acknowledge generous grants of computing time from Hokkaido University Computing Center.

References

1) A. Rhaman, *Phys. Rev.A*, **136**, 405 (1964).
2) D. Levesque and L. Verlet, *Phys. Rev. A*, **2**, 2514 (1970); D. Levesque, L. Verlet, and J. Kurkijarvi, *Phys. Rev. A*, **7**, 1690 (1973).
3) B. J. Alder and T. E. Wainwright, *Phys. Rev. Lett.*, **18**, 988 (1967); *Phys. Rev. A*, **1**, 18 (1970).

4) B. J. Alder, D. M. Gass, and T. E. Wainwright, *J. Chem. Phys.*, **53**, 3813 (1970).
5) J. P. Hansen and I. R. McDonald, "Theory of Simple Liquids," Academic Press, London (1976).
6) P. Schofield, "Statistical Mechanics," ed by K. Singer, Chem. Soc., London (1975), Vol. II.
7) S. Yip, *Ann. Phys. Chem.*, **30**, 547 (1979).
8) J. A. Barker and D. Henderson, *Rev. Mod. Phys.*, **48**, 587 (1976).
9) K. Arakawa, "Kagaku Sosetsu, No. 11, Ions and Solvents," (1976), p. 13.
10) J. H. Dymond and B. J. Alder, *J. Chem. Phys.*, **45**, 2061 (1966).
11) S. H. Chen and A. Rahman, *Mol. Phys.*, **34**, 1247, (1977); S. W. Haan, R. D. Mountain, C. S. Hsu, and A. Rahman *Phys. Rev. A*, **22**, 767 (1980).
12) D. Schiff, *Phys. Rev.*, **186**, 151 (1969).
13) In usual molecular dynamics studies of simple liquids, calculations have been made for the range of temperatures above the triple point of Ar, $T^*=0.70$. For the liquids composed of molecules with a comparatively strong interaction, if (ε/k) is assumed to be 500 K for example,[14] we have $T^*=0.6$ when $T=300$ K. In this paper, computations for $T^*=0.6$ are reported, and also some results for $T^*=1.0$ and 4.0 are given in Fig. 3, Fig. 10, and Table 1.
14) J. O. Hirschfelder, C. F. Curtiss, and R. B. Bird, "Molecular Theory of Gases and Liquids," Wiley, New York (1954).
15) L. Verlet, *Phys. Rev.*, **159**, 98 (1967).
16) B. J. Alder and C. E. Hecht, *J. Chem. Phys.*, **50**, 2032 (1969).
17) Y. Hiwatari, H. Matsuda, T. Ogawa, N. Ogita, and A. Ueda, *Prog. Theor. Phys.*, **52**, 1105 (1974).
18) L. Verlet, *Phys. Rev.*, **165**, 201 (1968).
19) R. Zwanzig and N. K. Ailawadi, *Phys. Rev.*, **182**, 280 (1969).
20) At lower densities, the agreement between the computed and predicted values is not good. This discrepancy is supposed to come from the effect of the attractive part of the potential, enhancing the correlation of the nearest neighbors at low densities.
21) S. A. Rice and P. Gray, "The statistical Mechanics of Simple Liquids," Wiley, New York (1965).
22) P. Schofield, "Molecular Motions in Liquids," ed by J. Lascombe, D. Reidel Publishing Co., Dordrecht, Holland (1974).
23) The binary collision time in force autocorrelation functions was discussed by Schofield *et al.* See Ref. 22.
24) J. P. J. Michels and N. J. Trappeniers, *Chem. Phys. Lett.*, **33**, 195 (1975).
25) T. Einwohner and B. J. Alder, *J. Chem. Phys.*, **49**, 1458 (1968).
26) W. T. Ashurst and W. G. Hoover, *Phys. Rev. A*, **11**, 658 (1975).
27) The effective potential theory due to Davis[28] incorporates the desirable features of the Rice-Allnatt theory, and is believed to be free from its several deficiencies. The contribution $\zeta^{H}_{*(3)}$ in the Davis expression is very small (of the order of 1—0.1% for the present case), however, so that the Davis theory gives essentially the same numerical results as the Rice-Allnatt theory.
28) H. T. Davis, *Adv. Chem. Phys.*, **24**, 257 (1973).
29) E. Helfand, *Phys. Fluids*, **4**, 681 (1961).
30) Another choice of $g(r)$ is to use the molecular dynamics values for the modified potential, Eq. 18. From this calculation the contact value of $g(r)$ is somewhat larger than that for the unmodified potential.
31) H. C. Longuet-Higgins and B. Widom, *Mol. Phys.*, **8**, 549 (1964).